PRAMANA
— journal of
physics

Vol. 72, No. 2
February 2009
pp. 343–353

Equilibrium and pre-equilibrium emissions in proton-induced reactions on ^{203,205}Tl

A KAPLAN[1], A AYDIN[2,*], E TEL[3] and B ŞARER[3]
[1]Faculty of Arts and Sciences, Süleyman Demirel University, 32260, Isparta, Turkey
[2]Faculty of Arts and Sciences, Kirikkale University, 71450, Kirikkale, Turkey
[3]Faculty of Arts and Sciences, Gazi University, 06500 Ankara, Turkey
[*]Corresponding author. E-mail: aaydin@kku.edu.tr

MS received 16 May 2008; revised 21 August 2008; accepted 26 August 2008

Abstract. In this study, the excitation functions for the reactions ^{203}Tl$(p,n)^{203}$Pb, ^{205}Tl$(p,3n)^{203}$Pb, ^{203}Tl$(p,2n)^{202}$Pb, ^{205}Tl$(p,4n)^{202}$Pb, ^{203}Tl$(p,3n)^{201}$Pb, ^{205}Tl$(p,5n)^{201}$Pb, ^{203}Tl$(p,4n)^{200}$Pb and ^{205}Tl$(p,6n)^{200}$Pb have been calculated using pre-equilibrium and equilibrium reaction mechanisms. Calculated results based on hybrid model, geometry-dependent hybrid model and cascade-exciton model have been compared with the experimental data.

Keywords. ^{203,205}Tl; pre-equilibrium reactions; exciton model; proton cyclotron.

PACS Nos 24.10.-i; 25.40.-h; 29.20.dg

1. Introduction

Recently, many experimental techniques have been developed to obtain and detect neutrons and charged particles of different energies and to measure the cross-sections of different particle-induced reactions [1]. Therefore, the neutron- and proton-induced nuclear reaction cross-section data are very important for several technical applications. The neutron-induced nuclear reaction cross-section data are necessary for the domain of fission-reactor technology for the calculation of nuclear transmutation rates, nuclear heating, radiation damage etc. The proton-induced nuclear reaction cross-section data are very important for the production of medical radioisotopes using cyclotrons [2–5]. Nuclear data evaluation is generally carried out on the basis of experimental data and theoretical model calculations. It is both practically and economically impossible to measure necessary cross-sections for all the isotopes in the periodic table for a wide range of energies. Nuclear reaction models are frequently needed to provide estimates of the particle-induced reaction cross-sections, especially if the experimental data are not available or unable to measure the cross-sections due to the experimental difficulty. Therefore, nuclear reaction model calculations play an important role in the nuclear data evaluation.

Table 1. The Q-values, threshold energies and optimum energy ranges for $^{203,205}\mathrm{Tl}(p, xn)$ reactions.

Reaction	Residual nucleus	Half-life and decay mode	Q-value (MeV)	Threshold energy (MeV)	Optimum energy range (MeV)
$^{203}\mathrm{Tl}(p, n)$	$^{203}\mathrm{Pb}$	51.9 h (EC)	−1.757	1.766	15–20
$^{205}\mathrm{Tl}(p, 3n)$			−15.960	16.037	25–35
$^{203}\mathrm{Tl}(p, 2n)$	$^{202}\mathrm{Pb}$	0.05 My (EC)	−8.681	8.724	15–25
$^{205}\mathrm{Tl}(p, 4n)$			−22.883	22.996	35–45
$^{203}\mathrm{Tl}(p, 3n)$	$^{201}\mathrm{Pb}$	9.3 h (EC)	−17.428	17.515	25–35
$^{205}\mathrm{Tl}(p, 5n)$			−31.630	31.786	40–60
$^{203}\mathrm{Tl}(p, 4n)$	$^{200}\mathrm{Pb}$	21.5 h (EC)	−24.514	24.636	40–50
$^{205}\mathrm{Tl}(p, 6n)$			−38.716	38.907	55–65

Besides, these obtained data are necessary to develop more nuclear theoretical calculation models in order to explain nuclear reaction mechanisms and the properties of the excited states in different energy ranges.

In the present paper, using equilibrium and pre-equilibrium reaction mechanisms, the (p, xn) cross-section values for ^{203}Tl and ^{205}Tl target nuclei were investigated in a range of 10–100 MeV incident energy. Equilibrium and pre-equilibrium particle emissions during the decay process of a compound nucleus are very important for a better understanding of the nuclear reaction mechanism induced by medium energy particles. The highly excited nuclear system produced by charged particles first decays by emitting fast nucleons at the pre-equilibrium (PE) stage and later on by the emission of low-energy nucleons at the equilibrium (EQ) stage.

Thallium has two odd-mass stable isotopes with different abundances (^{203}Tl (29.52%) and ^{205}Tl (70.48%)). Furthermore, its activation in some cases gives the same residual nucleus through different reaction channels, but very different Q-values and threshold energies, as seen in table 1. Contributions of equilibrium and pre-equilibrium reaction mechanisms have been investigated using different reaction model calculations. The excitation functions for the reactions $^{203}\mathrm{Tl}(p, n)^{203}\mathrm{Pb}$, $^{205}\mathrm{Tl}(p, 3n)^{203}\mathrm{Pb}$, $^{203}\mathrm{Tl}(p, 2n)^{202}\mathrm{Pb}$, $^{205}\mathrm{Tl}(p, 4n)^{202}\mathrm{Pb}$, $^{203}\mathrm{Tl}(p, 3n)^{201}\mathrm{Pb}$, $^{205}\mathrm{Tl}(p, 5n)^{201}\mathrm{Pb}$, $^{203}\mathrm{Tl}(p, 4n)^{200}\mathrm{Pb}$ and $^{205}\mathrm{Tl}(p, 6n)^{200}\mathrm{Pb}$ were calculated. The excitation functions for pre-equilibrium calculations were newly calculated using hybrid model, geometry-dependent hybrid model and cascade-exciton model. The reaction equilibrium component was performed using the Weisskopf–Ewing model [6]. Calculation results have been also compared with the available excitation function measurements in literature.

2. Basic calculation methods of cascade exciton model

The cascade–exciton model (CEM) combines essential features of the intranuclear cascade (INC) model with the exciton model. The CEM assumes that the reactions occur in three stages: INC, pre-equilibrium and equilibrium (or compound

nucleus). In the intranuclear cascade step, incident particle interacts with the target nucleus through successive nucleon–nucleon hard collisions leading to the emission of high energy nucleons. After the intranuclear cascade stage of the reaction the nucleus is left in an excited state. This is the starting point for the second or pre-equilibrium stage of the reaction. In the evaporation phase of the reaction, the remaining nucleus de-excites either by evaporation or by fission. The cascade stage of interaction is described by the Dubna version of the intranuclear cascade model [7–9] and the subsequent interaction states are considered in terms of the exciton model of pre-equilibrium decay which includes the description of the equilibrium evaporative third stage of the reaction [9]. Generally, these three components may contribute to any experimentally measured quantity. In particular, for the inclusive particle spectrum [7], we have

$$\sigma(p)\mathrm{d}p = \sigma_{\mathrm{in}}[N^{\mathrm{cas}}(p) + N^{\mathrm{prq}}(p) + N^{\mathrm{eq}}(p)]\mathrm{d}p, \tag{1}$$

where p is a linear momentum, N^{cas}, N^{prq} and N^{eq} are respectively the cascade, the pre-equilibrium and the equilibrium components. The inelastic cross-section σ_{in} is not taken from the experimental data or independent optical model calculations, but it is calculated within the cascade model itself. Hence the CEM predicts the absolute values for calculated characteristics and does not require any additional data or special normalization of its results.

3. Basic calculation methods of hybrid and geometry-dependent hybrid model

The hybrid model for pre-compound decay is formulated by Blann and Vonach [10] as

$$\begin{aligned}\frac{\mathrm{d}\sigma_\nu(\varepsilon)}{\mathrm{d}\varepsilon} &= \sigma_{\mathrm{R}} P_\nu(\varepsilon)\\ P_\nu(\varepsilon)\mathrm{d}\varepsilon &= \sum_{\substack{n=n_0\\ \Delta n=+2}}^{\bar{n}} \bar{n}[{}_n\chi_\nu N_{\mathrm{n}}(\varepsilon, U)/N_{\mathrm{n}}(E)]g\,\mathrm{d}\varepsilon\\ &\quad\times[\lambda_{\mathrm{c}}(\varepsilon)/(\lambda_{\mathrm{c}}(\varepsilon) + \lambda_+(\varepsilon))]D_{\mathrm{n}},\end{aligned} \tag{2}$$

where σ_{R} is the reaction cross-section, ${}_{\mathrm{n}}\chi_\nu$ is the number of particle type ν (proton or neutron) in n exciton hierarchy, $P_\nu(\varepsilon)\mathrm{d}\varepsilon$ represents number of particles of the ν (neutron or proton) emitted into the unbound continuum with channel energy between ε and $\varepsilon + \mathrm{d}\varepsilon$. The quantity in the first set of square brackets of eq. (2) represents the number of particles to be found (per MeV) at a given energy ε for all scattering processes leading to an n exciton configuration. $\lambda_{\mathrm{c}}(\varepsilon)$ is the emission rate of a particle into the continuum with channel energy ε and $\lambda_+(\varepsilon)$ is the intranuclear transition rate of a particle. It has been demonstrated that the nucleon–nucleon scattering energy partition function $N_{\mathrm{n}}(E)$ is identical to the exciton state density $\rho_{\mathrm{n}}(E)$, and may be derived by certain conditions on N–N (nucleon–nucleon) scattering cross-sections [10,11]. The second set of square brackets in eq. (2) represents the fraction of the ν type particles at an energy which should undergo emission

into the continuum, rather than making an intranuclear transition. D_{n} represents the average fraction of the initial population surviving to the exciton number being treated.

The intranuclear cascade calculation results indicated that the exciton model deficiency resulted from a failure to properly reproduce enhanced emission from the nuclear surface [10]. In order to provide a first-order correction for this deficiency the hybrid model was reformulated by Blann and Vonach [10]. In this way the diffuse surface properties sampled by the higher impact parameters were crudely incorporated into the pre-compound decay formalism, in the geometry-dependent hybrid model (GDH). The differential emission spectrum is given in the GDH as

$$\frac{\mathrm{d}\sigma_\nu(\varepsilon)}{\mathrm{d}\varepsilon} = \pi\lambda\!\!\!^{-2}\sum_{l=0}^{\infty}(2l+1)T_l P_\nu(l,\varepsilon) \tag{3}$$

where $\lambda\!\!\!^{-}$ is the reduced de Broglie wavelength of the projectile and T_l represents transmission coefficient for the lth partial wave. Using the total pre-compound neutron emission spectrum $\mathrm{d}\sigma_{\mathrm{n}}(\varepsilon)/\mathrm{d}\varepsilon$, the cross-section which could be involved in the emission of two neutrons is calculated as $\sigma_{2\mathrm{n}} = \int_{U=0}^{E-B_{2\mathrm{n}}}(\mathrm{d}\sigma_{\mathrm{n}}(\varepsilon)/\mathrm{d}\varepsilon)\mathrm{d}\varepsilon$, where $B_{2\mathrm{n}}$ represents the sum of the first and the second neutron binding energies.

The geometry-dependent influences are manifested in two distinct manners in the formulation of the GDH model. The more obvious is the longer mean free path predicted for nucleons in the diffuse surface region. The second effect is less physically secure, yet seems to be important in reproducing experimental spectral shapes.

4. Basic calculation methods of equilibrium model

Equilibrium emission is calculated according to Weisskopf–Ewing (WE) model [6] neglecting angular momentum. In the evaporation, the basic parameters are binding energies, inverse reaction cross-section, the pairing and the level-density parameters. The reaction cross-section for incident channel a and exit channel b can be written as

$$\sigma_{ab}^{\mathrm{WE}} = \sigma_{ab}(E_{\mathrm{inc}})\frac{\Gamma_b}{\sum\limits_{b'}\Gamma_{b'}}, \tag{4}$$

where E_{inc} is the incident energy, $\Gamma_b = \frac{2_{s_b}+1}{\pi^2\hbar^2}\mu_b\int \mathrm{d}\varepsilon\sigma_b^{\mathrm{inv}}(\varepsilon)\varepsilon\frac{\omega_1(U)}{\omega_1(E)}$, U is the excitation energy of the residual nucleus, μ_b is the reduced mass, s_b is the spin and the total single-particle level density is taken as

$$\omega_1(E) = \frac{1}{\sqrt{48}}\frac{\exp[2\sqrt{\alpha(E-D)}]}{E-D}; \quad \alpha = \frac{6}{\pi^2}g, \tag{5}$$

where σ_b^{inv} is the inverse reaction cross-section, E is the excitation energy of the compound nucleus, D is the pairing energy and g is the single particle level density.

5. Calculations and analysis

The present paper describes new calculations on the excitation functions of ^{203}Tl$(p,n)^{203}$Pb, ^{205}Tl$(p,3n)^{203}$Pb, ^{203}Tl$(p,2n)^{202}$Pb, ^{205}Tl$(p,4n)^{202}$Pb, ^{203}Tl$(p,3n)^{201}$Pb, ^{205}Tl$(p,5n)^{201}$Pb, ^{203}Tl$(p,4n)^{200}$Pb and ^{205}Tl$(p,6n)^{200}$Pb reactions carried out in the 10–100 MeV proton incident energy range.

In the calculations, the codes ALICE/ASH [12] and CEM95 [8] have been used. The pre-equilibrium calculations on the excitation functions were carried out with ALICE/ASH computer code [12] for hybrid model and the geometry-dependent hybrid model, and CEM95 computer code [8] for cascade exciton model. And also the reaction equilibrium component in ALICE/ASH computer code is done using a traditional compound nucleus model of Weisskopf and Ewing [6]. The ALICE/ASH code is an advanced and modified version of the ALICE-91 code [13]. The ALICE/ASH code can be applied for the calculation of excitation functions, energy and angular distribution of secondary particles in nuclear reactions induced by nucleons and nuclei up to an energy range of 300 MeV. The generalized superfluid nuclear model [14] has been applied for nuclear level density calculations in the ALICE/ASH code. Model parameters were taken from ref. [15]. We used the initial exciton number as $n_0 = 3$ (1 proton, 1 neutron and 1 hole). A detailed description of the ALICE/ASH code can be found in ref. [12].

Other calculations have been made in the framework of cascade–exciton model (CEM) by making use of CEM95 code [8] with the level density parameter using the systematic of Iljinov *et al* [16]. A detailed description of the CEM95 can be found in ref. [8].

5.1 *Production of* ^{203}*Pb*

There is no experimental data for ^{203}Tl$(p,n)^{203}$Pb reaction. Therefore, we have given only theoretical calculations in figure 1. The calculation for the excitation function of ^{205}Tl$(p,3n)^{203}$Pb reaction is compared with the reported experimental values in figure 5 [17]. The pre-equilibrium calculations (hybrid and GDH models) and cascade-exciton model calculations are in good agreement with the experimental data. Also, the equilibrium calculations are in good agreement with the measurements up to 35 MeV. The optimum energy range for the production of ^{203}Pb (in ^{205}Tl$(p,3n)^{203}$Pb reaction) is $E_p = 35 \rightarrow 20$ MeV, and so this process can be employed in a small cyclotron.

5.2 *Production of* ^{202}*Pb*

There is no experimental data for ^{203}Tl$(p,n)^{203}$Pb reaction, and therefore we have given only theoretical calculations in figures 2 and 6.

5.3 *Production of* ^{201}*Pb*

The calculated excitation functions of ^{203}Tl$(p,3n)^{201}$Pb and ^{205}Tl$(p,5n)^{201}$Pb reactions are compared with the experimental values in figures 3 and 7. High

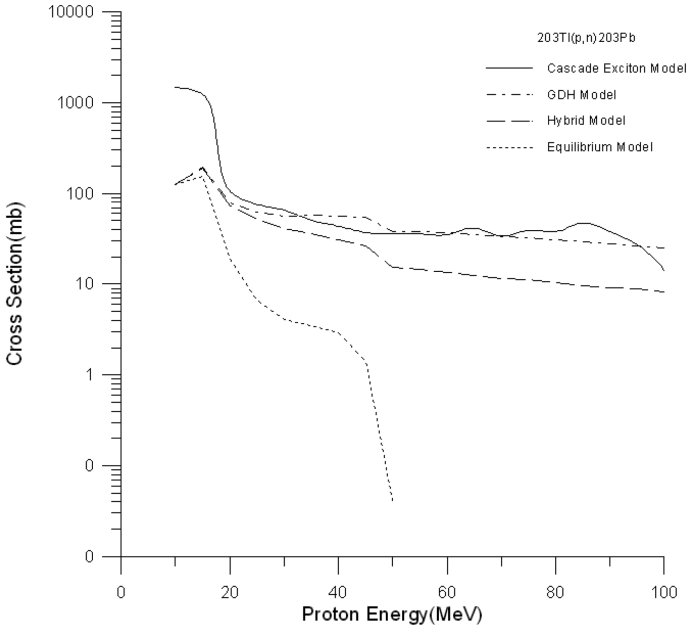

Figure 1. The comparison of calculated excitation functions of $^{203}\mathrm{Tl}(p,n)^{203}\mathrm{Pb}$ reaction. No experimental data are reported in literature.

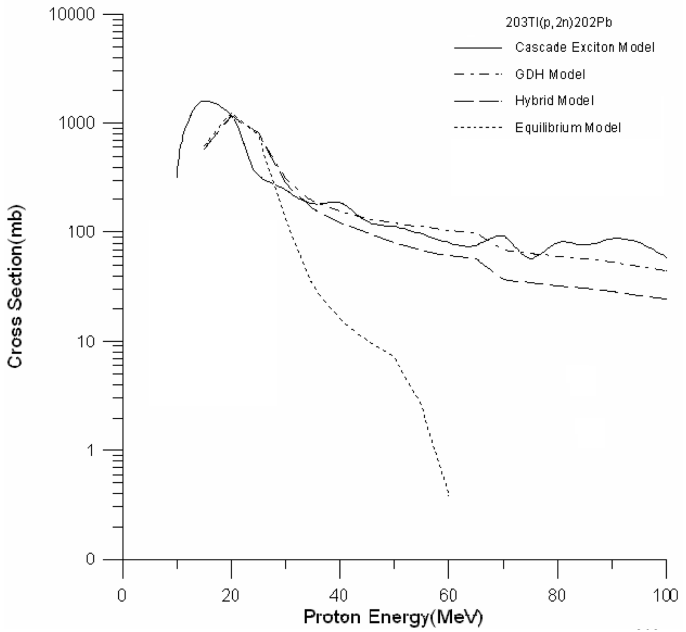

Figure 2. The comparison of calculated excitation functions of $^{203}\mathrm{Tl}(p,2n)^{202}\mathrm{Pb}$ reaction. No experimental data are reported in literature.

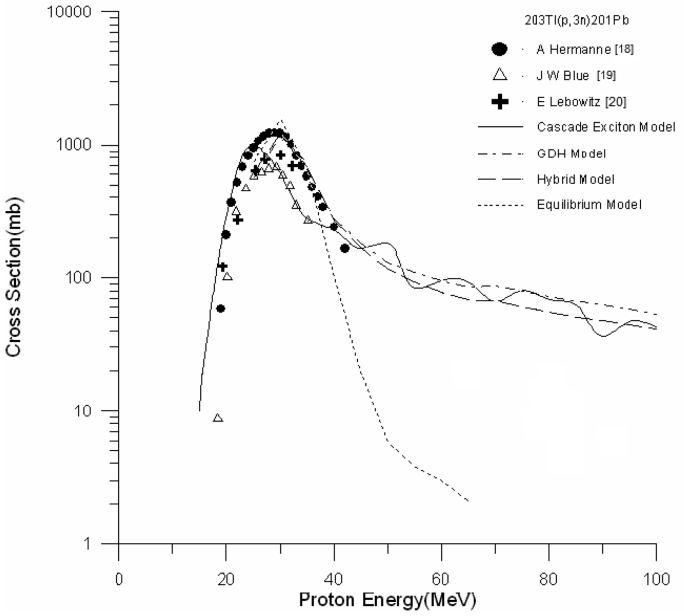

Figure 3. The comparison of calculated excitation functions of $^{203}\mathrm{Tl}(p,3n)^{201}\mathrm{Pb}$ reaction with the values reported in literature.

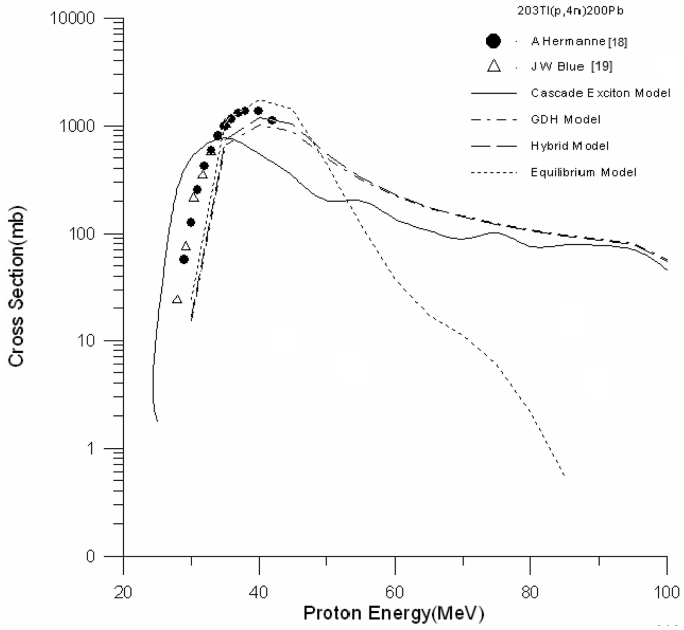

Figure 4. The comparison of calculated excitation functions of $^{203}\mathrm{Tl}(p,4n)^{200}\mathrm{Pb}$ reaction with the values reported in literature.

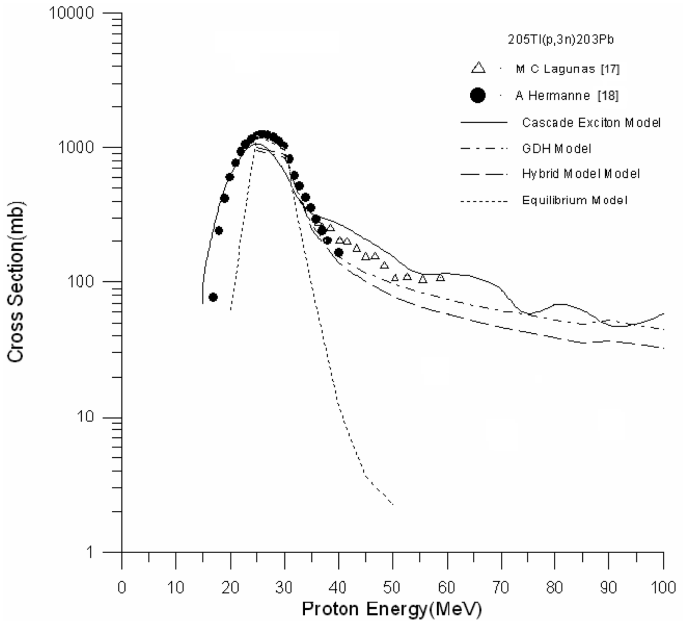

Figure 5. The comparison of calculated excitation functions of $^{205}\mathrm{Tl}(p,3n)^{203}\mathrm{Pb}$ reaction with the values reported in literature.

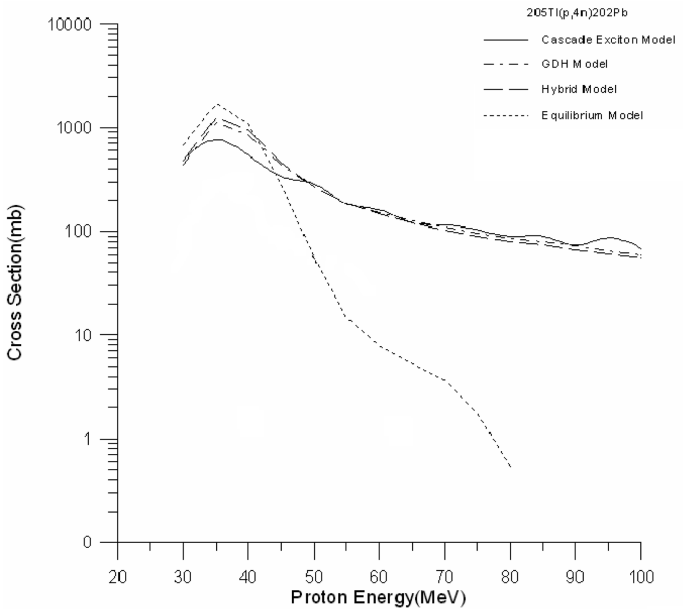

Figure 6. The comparison of calculated excitation functions of $^{205}\mathrm{Tl}(p,4n)^{202}\mathrm{Pb}$ reaction. No experimental data are reported in literature.

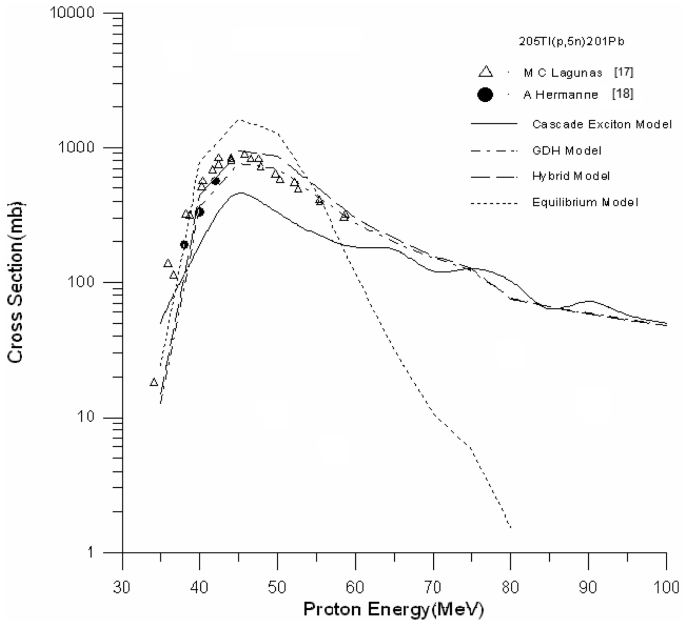

Figure 7. The comparison of calculated excitation functions of $^{205}\mathrm{Tl}(p,5n)^{201}\mathrm{Pb}$ reaction with the values reported in literature.

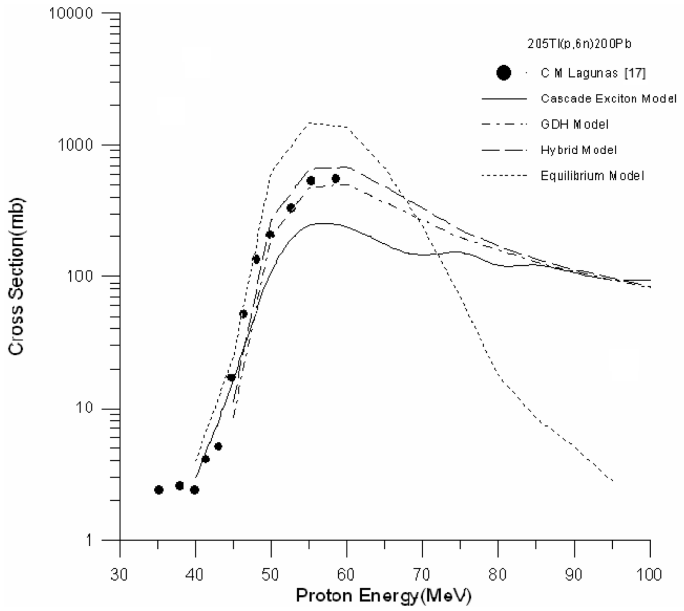

Figure 8. The comparison of calculated excitation functions of $^{205}\mathrm{Tl}(p,6n)^{200}\mathrm{Pb}$ reaction with the values reported in literature.

discrepancies are observed in experimental data for ^{203}Tl$(p, 3n)^{201}$Pb reaction. The pre-equilibrium calculations (hybrid and GDH models) are in good agreement with the measurements of Hermanne *et al* [18]. The cascade exciton model calculations (CEM95) are in good agreement with the experimental values of Blue *et al* [19] and Lebowitz *et al* [20]. For ^{205}Tl$(p, 5n)^{201}$Pb reaction, the pre-equilibrium calculations (hybrid and GDH models) are in good agreement with the measurements. In the energy region between 40 and 45 MeV, the equilibrium calculations give high results. Also the cascade exciton model calculations (CEM95) are lower than the experimental values.

5.4 *Production of* ^{200}*Pb*

The calculated excitation functions of ^{203}Tl$(p, 4n)^{200}$Pb and ^{205}Tl$(p, 6n)^{200}$Pb reactions are compared with the experimental values in figures 4 and 8. The equilibrium calculations of ^{203}Tl$(p, 4n)^{200}$Pb reaction are in good agreement with the measurements between 30 and 40 MeV. For ^{205}Tl$(p, 6n)^{200}$Pb reaction the pre-equilibrium calculations (hybrid and GDH models) are in good agreement with the measurements. In the energy region above 45 MeV, the equilibrium calculations give too high results. The cascade-exciton model calculations (CEM95) are in good agreement with the experimental values at energies below 45 MeV.

6. Conclusions

In the present paper, using equilibrium and pre-equilibrium reaction mechanisms, the (p, xn) cross-section values for ^{203}Tl and ^{205}Tl target nuclei have been calculated for 10–100 MeV incident energy ranges.

The calculation results on the excitation functions and the optimum energy ranges for reaction process are given in figures 1–8 and table 1. Generally the new model calculations used for all reactions are in good agreement with the measurement data. Also as can be seen in figures 1–8, the high energy part of the experimental excitation functions cannot account for by the equilibrium decay mechanism and the pre-equilibrium emission must be considered along with compound nucleus decay. Besides, the pre-equilibrium effects increase as the incident energy increases. The results of this study are in good agreement with the earlier investigations [5,21–24].

Acknowledgment

This work has been supported by State Planning Organization of Turkey project DPT-2006K # 120470. The authors would like to thank C H M Broeders, A Yu Konobeyev, Yu A Korovin, V P Lunev, M Blann for supporting ALICE/ASH-code.

References

[1] R A Forrest, J Kopecky and J-Ch Sublet, The European Activation File: EAF-2005 Cross Section Library, UKAEA FUS 515 (2005)

[2] S M Qaim, *J. Nucl. Sci. Technol.* **2**, 1272 (2002)
[3] S M Qaim, *Radiat. Phys. Chem.* **71**, 917 (2004)
[4] S M Qaim, F Tarkanyi, P Oblozinsky, K Gul, A Hermanne, M G Mustafa, F M Nortier, B Scholten, Y N Shubin, S Takacs and Y Zhuang, *J. Nucl. Sci. Tech.* **2**, 1282 (2002)
[5] A Aydin, B Şarer and E Tel, *Appl. Radiat. Isot.* **65**, 365 (2007)
[6] V F Weisskopf and D H Ewing, *Phys. Rev.* **57**, 472 (1940)
[7] K K Gudima, S G Mashnik and V D Toneev, *Nucl. Phys.* **A401**, 329 (1983)
[8] S G Mashnik, User Manual for the Code CEM95, Joint Institute for Nuclear Research, Dubna, Moscow Region (1995)
[9] S G Mashnik and V D Toneev, Communications of the Joint Institute for Nuclear Research, P4-8417 (Dubna, 1974)
[10] M Blann and H K Vonach, *Phys. Rev.* **C28**, 1475 (1983)
[11] M Blann, A Mignerey and W Scobel, *Nukleonika* **21**, 335 (1976)
[12] C H M Broeders, A Yu Konobeyev, Yu A Korovin, V P Lunev and M Blann, ALICE/ASH – pre-compound and evaporation model code system for calculation of excitation functions, energy and angular distributions of emitted particles in nuclear reactions at intermediate energies, FZK 7183, May 2006, http://bibliothek.fzk.de/zb/berichte/FZKA7183.pdf
[13] M Blann, Code ALICE-91, PSR-146, Statistical Model Code System with Fission Competition, Oak Ridge National Laboratory, RSICC Peripheral Shielding Routine Collection, Lawrence Livermore National Laboratory, Livermore, California and IAEA
[14] A V Ignatyuk, K K Istekov and G N Smirenkin, *Yadernaja Fizika* **29**, 875 (1979)
[15] A V Ignatyuk, in: *Handbook for calculations of nuclear reaction data*, IAEA-TECDOC-1034, International Atomic Energy Agency Report, 1998, p. 65, http://www.nds.iaea.or.at/ripl/ripl_handbook.htm
[16] A S Iljinov, M V Mebel, N Bianchi, E De Sanctis, C Guaraldo, V Lucherini, M Muccifora, E Polli, A R Reolon and P Rossi, *Nucl. Phys.* **A543**, 517 (1992)
[17] M C Lagunas-Solar, J A Jungerman and D Paulson, http://www.nndc.bnl.gov/exfor7/, EXFOR: # A0180 (1980)
[18] A Hermanne, N Walravens and O Cicchelli, http://www.nndc.bnl.gov/exfor7/, EXFOR: #A0494 (1991)
[19] J W Blue, D C Liu and J B Smathers, http://www.nndc.bnl.gov/exfor7/, EXFOR: #C1027 (1978)
[20] E Lebowitz, M W Greene, R Fairchild, P R Bradley-Moore, H L Atkins, A N Ansari, P Richards, E Belgrave, http://www.nndc.bnl.gov/exfor7/, EXFOR: #C1028 (1975)
[21] N P Sathik, M A Ansari, B P Singh, M Ismail and M H Rashid, *Phys. Rev.* **C66**, 14602 (2002)
[22] E Tel, Ş Okuducu, A Aydin, B Şarer and G Tanir, *Acta Phys. Slov.* **54(2)**, 191 (2004)
[23] B Şarer, M Gunay, A Aydin, E Tel and A Arasoglu, *Nucl. Sci. Eng.* **153(2)**, 192 (2006)
[24] A Aydin, E Tel and B Şarer, *Phys. Scr.* **75**, 299 (2007)